A COMPARATIVE LABORATORY AND FULL-SCALE STUDY OF THE NEAR WAKE STRUCTURE OF A WIND TURBINE

C.G. Helmis[1] , J. Whale[2] , K.H. Papadopoulos[1], C.G. Anderson[2], D.N. Asimakopoulos[1] and D.J. Skyner[2]

1 University of Athens, GREECE
2 University of Edinburgh, SCOTLAND

INTRODUCTION

The operation of a wind turbine produces a downstream region of reduced wind speed, the so-called wake. The wake constitutes an important factor in determining the siting of turbines in wind farms. The mean wake characteristics, and their relation to the incident wind field and the local topography, are of primary importance for the estimation of available wind energy. The turbulent structure of the wake affects the loading and fatigue of downstream turbine rotors, and dictates the minimum spacing of the machines within a wind farm. In order, then, to achieve satisfactory performance from wind farms, especially in areas of complex terrain, a detailed knowledge of the above wake parameters is required.

The present paper describes a recent investigation into the properties of the wake of a three-bladed wind turbine. Measurements were made on both a full-scale machine, and on a replica model in the laboratory, at approximately 1/100 scale. The full-scale experiments were carried out on the Greek island of Samos, by workers from the University of Athens, and were based on comprehensive anemometry measurements. The small-scale experiments were conducted by a research group at the University of Edinburgh, Scotland, using the relatively new technique of particle image velocimetry (PIV).

A major objective of the work was to assess the validity of small-scale PIV measurements as a tool for investigating full-scale wind turbine phenomena. If successful, there would be significant attractions in using the PIV method, due to its ability to map the velocity in the entire rotor wake at a given instant. PIV vector maps may be processed to yield both bulk wake measurements, such as velocity deficits, or data relating to the detailed structure of the wake, e.g. vorticity measurements. In the present campaign, velocity ratios measured 1.1 diameters (D) downstream of the rotor, ie. in the near wake, were compared, using data from full-scale and model scale.

REVIEW OF PREVIOUS WORK

Field studies of wakes behind single turbines or of multiple wakes in wind farms [Hogstrom et al (1), Taylor et al (2), Larsen and Velk (3), Nierenberg (4), Elliot and Barnard (5)] usually concentrate on the decay rate of the velocity deficits in the far-wake region. This is then related to power production optimization of wind farms. While confirming the qualitative trends revealed by wind tunnel simulations, field studies have indicated the necessity of further measurements, especially over complex terrain [Van der Snock (6)], in order to improve the proposed models.

Wind tunnel studies have demonstrated that the simulated near wake region, which is usually described by a uniform velocity profile in the so-called potential core, is not an accurate representation of the real-flow situation [Ainslie (7)]. This suggests that the effect of the turbulence produced by the turbine is improperly parameterized.

Measurements at distances as close as 1D downstream are rare, although of importance. The few examples include the comprehensive wind tunnel study of Papaconstantinou and Bergeles (8), the extended Nibe project [Taylor (9)] which included some experimental results at 1D and the study of the near wake structure of a Darrieus turbine by Strickland and Goldman (10).

The use of PIV in wind turbine studies is a recent development. Infield et al (11) have applied the technique both in the wind tunnel, and to a full-scale wind turbine in the field. Their studies concentrated on the immediate vicinity of the blade, and produced detailed profiles of bound circulation and the tip vortex.

Visualisation of the full wake of the rotor up to 4D downstream was achieved at Edinburgh [Whale and Anderson (12)] using a small scale model, with water, rather than air, as the flow medium.

EXPERIMENTS

Full-Scale Measurements

Experimental layout. The full-scale tests were carried out on Samos Island, which lies in the eastern region of the Aegean Sea. The wind farm on Samos is located 390m above mean sea level on a saddle confined by the island's two major mountain ranges. The wind park comprises nine three-bladed, horizontal-axis, Vestas WM19S wind turbines, with rotor diameter of 19 m, hub-height of 25 m, and output rating of 100 kW.

The WM19S is stall-regulated, with rated power achieved at a windspeed of 13 m/s. The cut-in and cut-out wind speeds are 3 m/s and 27 m/s, respectively. The blades'

rotational speed is 48 RPM, and the maximum power coefficient C_{pmax} of 0.38 is attained in the windspeed range 8-10 m/s.

Measurements were made on a single wind turbine, using two fully instrumented meteorological masts, one upwind (0.8D) and one downwind (1.1D) of the machine. The data to be compared refer to two cup anemometers, mounted at 12m and 29m above ground level, on the upwind and downwind mast, respectively. At the given elevation (29m), the downstream unit was above the centreline of the rotor, well clear of the influence of downstream tower shadow. The experimental layout is described fully by Helmis et al (13).

The measurements were made over the period 16-24/8/91; the anemometers were sampled at a rate of 1Hz.

The wake velocity was expressed as the ratio of downstream to upstream windspeed. In doing this, it was necessary to compensate for influences other than the wind turbine wake: these were principally wind shear, non-uniform inflow conditions due to the local terrain, and downstream tower shadow (as noted above, however, the last of these was effectively removed by analysing data at a downstream elevation in the upper half of the wake). Measurements were therefore taken with the turbine in operation (the wake data set) and stationary (the non-wake data set). The results in the latter case (Fig. 1) were used to establish two correction curves (for low and high wind speeds) for non-wake effects.

Results and analysis. A preliminary analysis of the non-wake data set was used to establish the background correction to be applied to operational data. The importance of this procedure is seen from previous results described in (13), who highlight the uncertainty introduced by estimating wake velocity deficits by comparing upstream and downstream measurements using data recorded only with the turbine in operation.

The background correction is particularly important when dealing with the near-wake region. In complex topography this is due to terrain inhomogenities; below hub-height the effects of nacelle and tower shadow are also important (2).

The non-wake velocity ratio was found to vary significantly with wind direction. Non-wake data for low and high wind speeds were therefore used to yield two correction curves, which gave the non-wake velocity ratio as a function of wind direction only for the particular wind speed range. This was then used to provide correction factors for the data obtained during operation of the turbine: a given velocity ratio obtained with the turbine running was divided by the non-wake ratio corresponding to the same incident wind direction. In this way the effects of topography and wind shear were removed.

It should also be said that, by normalising the wake velocity with respect to the upstream anemometer readings (suitably corrected), it is implied that the upstream values of wind speed and ambient turbulence are considered representative of the actual flow which intersects the rotor. In fact, separate analysis verified that the wind speed and turbulence intensity were fairly constant through the rotor disk. The observed ranges for wind speed and turbulence intensity were 9-27 m/s and 3-16% respectively, based on 1-minute averages.

The corrected wake data, ie. with the turbine operational, are shown for a range of wind speeds in Fig. 2. The data are plotted against incident wind direction: on the assumption that the wind turbine yaw system tracks the wind direction accurately over long periods, the data can be re-interpreted as velocity-ratio profiles obtained by a horizontal traverse behind, and parallel to, the rotor.

Although full wake profiles are not available, due to a shortage of data, the results show a clear dependence on windspeed, with the wake deficit (defined as one minus the velocity ratio) increasing as a function of tip speed ratio. Assuming that the wake centreline corresponds with the 350deg wind direction, for which the wind turbine is directly upwind of the 29m measuring anemometer, centreline velocity ratios may be derived directly from the data in Fig. 2.

The given wake profiles are based on 1-min averages. Based on longitudinal and lateral coherence considerations performed in (9), it is concluded that the relatively short averaging time is appropriate. Analysis of corresponding 15-minute samples gives almost identical results, though with a somewhat more 'spiky' appearance: this was attributed to changes in rotor orientation during the 15-min period due to operation of the yaw system. The graphs based on 1-min data are nonetheless fairly smooth. The statistical significance of the results may be assumed greatest for the more extended wake data sets.

Note that the wake profiles thus obtained are inherently averaged with respect to short-term variations of incident wind direction. It is assumed that on the average the rotor was aligned with the incident upstream wind direction throughout the measurements (no turbine yaw information was available); it is to be expected, however, that rotor alignment lags behind changes in incident wind direction. The measured standard deviation of wind direction was ~5-6 deg, implying a maximum cross-wake smoothing over ±5% D.

Laboratory-scale measurements

Experimental method. The experiments at model scale were made using the technique of particle image velocimetry (PIV). PIV is a non-intrusive velocity measurement technique which allows two-dimensional flow fields to be captured at a single instant. The basis of PIV is to stroboscopically illuminate a two-dimensional plane of flow containing small, neutrally buoyant, seeding particles by means of a sheet of pulsed light. A double (or multiple) exposure photograph of this plane is taken; the spacing between the images of each particle on the film gives the local velocity. This photograph is then analysed to determine the local flow velocities across the whole field.

The film is interpreted point by point over a dense grid using a combination of optical and digital analysis: this involves scanning successive small regions of the negative with a probe laser to produce an interference pattern from the multiple particle images in that area. The interference

fringes are measured and recorded in digital form and the data Fourier transformed to yield the particle velocities at that point. The whole negative is scanned in this way to build up a flow velocity map, which forms the basis of all subsequent analysis.

The technique of PIV was introduced to the field of wind turbine aerodynamics by Infield et al (11) who conducted tests on a 0.9 m diameter wind turbine in a wind tunnel, using pulsed lasers. The tests established the applicability and usefulness of PIV as a velocimetry tool for wind turbines. The same researchers subsequently made PIV measurements on a full-scale wind turbine of 17 m diameter. These tests were mainly concerned with visualising the flow around a localised region of the blade, however. Visualisation of the entire wake at full scale using pulsed lasers presents obvious difficulties.

The PIV apparatus at Edinburgh University, which was used in the present study, is applicable to scale model rotors only, but is capable of capturing images from the near wake up to 4D downstream. The experiments were carried out in a two-dimensional water flume, 10 m long by 400 mm wide (Figure 3). The flume has glass walls and base, and was filled with water to a depth of 750 mm. A continuous current can be established in the tank, driven by a water pump, and returned via an external pipe system.

A continuous wave (CW) laser was used in conjunction with a scanning beam system of illumination to produce the laser sheet [Gray (14)].

The laser sheet was directed through the base of the flume, illuminating a two dimensional cross-section of the flow. The use of water as the flow medium greatly facilitates seeding and illumination. The model turbine rig was placed in the tank, with the rotor aligned normal to the incident flow. The water was seeded with conifer pollen of average diameter 70 μm; concentrations were maintained at a level that ensured a high density of non-overlapping particles on the resulting film record.

The model rotor was a 1/100th scale replica of the 3-bladed Vestas (formerly Windmatic) WM-19S. The blades were manufactured from rigid plastic, using a numerically controlled cutter. Despite the small scale, the model blades were accurately profiled with a NACA-632XX section, with twist, chord and thickness distributions based on the manufacturers' original drawings. In the tank, the turbine was driven by an electric motor suspended on a frame above the water level, and connected to the rotor shaft by a toothed belt, internal to an aluminium tube, effectively an inverted 'tower'. In order to reduce the disturbance to the rotor wake caused by the tower, it was streamlined with a foam plastic shroud of symmetric aerofoil cross-section.

The image recording equipment consisted of a rotating-mirror shifting system, and a Hasselblad camera. The purpose of the shifting system was to superpose a known velocity component onto the recorded image; the reasons for this were (a) to eliminate directional ambiguity in the final vector maps, and (b) to increase the dynamic range of the system. The shifting sequence was synchronized with an index pulse from a position encoder, connected to the turbine drive motor.

For reasons of geometry, the image shift-velocity was not constant over the entire field. A correction therefore had to be applied to the processed results, based on the relative positions of the camera, mirror and measurement area, the refractive indices of glass and water, and the spherical aberrations of the camera lens. This was done using appropriately written software; the estimated distortion in shift velocity from the centre of the film plane to the edges of the field was 9%.

Replicating full-scale conditions. The experiments were aimed at reproducing the full-scale measurements taken on Samos. Thus, the model was positioned so that the laser sheet intersected the blade at a location corresponding to the downstream anemometer unit at full scale (see above). The rotor centreline was positioned at a distance of 0.42R from the laser sheet, where R is the radius of the rotor. Assuming an axially symmetric wake, data were thus recorded at an equivalent offset position from the centre of the wake to the readings taken at full scale.

In order to simulate the desired velocity profile and turbulence level, turbulence manipulators were placed upstream of the rotor. These consisted of a parallel system of baffles comprising an aluminium honeycomb section, a perforated plate and a fine mesh (see Fig. 3).

The honeycomb acted as a flow straightener, with the perforated plate serving to impose a particular upstream profile. They were placed a number of mesh-lengths apart from each other and from the fine mesh to allow for turbulence introduced by their presence to decay. Final smoothing was provided by the fine mesh screen.

From the Samos experiments, it was concluded that the wind speed and turbulence intensity were fairly constant through the rotor disk. Thus, the turbulence manipulators in the water tank were chosen to produce a uniform upstream profile with low turbulence. A perforated plate with 32 mm diameter holes and regular pitch of 38 mm was placed 500 mm downstream of the honeycomb section. A fine mesh screen of 18 lines/inch was placed a further 800 mm downstream, 1200 mm upstream of the rotor.

As noted above, an important feature of this work was to establish whether tests on a rotor at model scale could yield valid data regarding the performance of full-scale wind turbines. Notwithstanding the size of the model, it was decided to replicate as accurately as possible the conditions pertaining to the full-scale measurements on Samos. In this way, any discrepancies between the full-scale measurements and those obtained from the PIV tests could be attributed solely to scale effects.

Geometric similarity between the model and the full-scale machine was ensured by the use of an accurate replica. Kinematic similarity during the tests was achieved by running the model at an appropriate range of tip speed ratios λ, using the motor speed controller. The current velocity was maintained constant throughout; initially, it was estimated from the valve settings of the recirculating pump, but final current values were derived from the PIV analysis.

CAPTION

TERMINATION

Because the full-scale results were based on time-averaged recordings, while the PIV vector maps corresponded to instantaneous wake images, it was necessary to introduce averaging in the latter case. This was done by repeating each PIV test several times, with the image synchronised to a different rotor position, and taking a numerical average of the resulting vector maps. In practice, the shifting sequence was synchronized to photograph the blades in 6 different azimuthal positions, 20deg apart. For a 3-bladed rotor, this discretizes one whole revolution. Post-analysis averaging of these 6 exposures yields six vector maps which, averaged together, provide the equivalent of a time-averaged wake image.

Results. The PIV photographs thus obtained were processed to yield two-dimensional velocity vector maps of the type shown in Fig. 4. This shows the wake behind the model rotor operating at a tip speed ratio of 6.5. Each vector indicates the velocity in the flow at that point: the area of reduced velocity behind the rotor is clearly seen in this image. Velocity maps were obtained at five tip speed ratios in the range 2.3-8.1.

The cross-wake profile at 1.1D downstream of the model rotor was found by analysing the single column of vectors in each map corresponding to the appropriate distance from the rotor. The results are shown in Fig. 5, as velocity ratio plotted against cross-wake distance. In calculating the velocity ratio for each location, a single averaged value of the upstream velocity was assumed: this was calculated from the mean flow statistics of the first column of vectors in the vector field, with corrections for the distortion introduced by image-shifting (see above).

Note that the vertical scales for the wake profiles have been shifted to separate them. The influence of tip speed ratio can be clearly seen from Fig. 5, with the downstream velocity ratio decreasing with increasing λ. The asymmetry seen in the profiles at their outer edges (where conditions approach those in the freestream) is attributed to the presence of the model support structure, ie. the 'tower' of the wind turbine. Despite its streamlined shroud, this evidently still introduces some turbulence behind the rotor disc.

From the given wake profiles, centreline velocity ratios may finally be obtained. As noted above, the wake ratios measured at full scale (Figure 2) incorporate directional smoothing, due to the variation in incident wind direction during the averaging period. To account for this at model scale, the centreline velocity at 1.1D downstream was averaged over a cross-wake distance based on the variance of the wind direction in the full scale tests. In practice, this involved averaging together the single centreline velocity vector at 1.1D downstream with the two adjacent (cross-wake) values.

The resulting centreline velocity ratios from the model tests are shown as a function of tip speed ratio in Fig. 6, together with the corresponding data from the Samos Island measurements. The correspondence is very encouraging. Note that the error bars attached to the model-scale results are based on the standard error of the cross-wake averaged centreline velocity ratios. As such, they reflect the level of turbulence existing at the location of interest in each case. It is noteworthy that the turbulence appears to increase towards both high and low tip speed ratios, with a minimum existing in between.

An explanation for this may be that at low tip speed ratio the rotor is heavily stalled, and the turbulence is due to the separated flow behind the individual blades of the model rotor; this may be referred to as 'local' turbulence. At high tip speed ratio the blades are likely to be largely unstalled, with smooth (unseparated) flow over their surfaces; however, by now the wake itself is highly turbulent on a large scale, due to the strong vorticity being transmitted into it from the rotor. At some intermediate value of tip speed ratio, the blades may be operating out of stall, but with a relatively weak vortex pattern in the wake. The spectral analysis of the full-scale data has already revealed fundamental variations of the turbulent structure of the near wake as the tip speed ratio varies [Helmis et al (15)].

Figure 7 contains a further comparison of the full-scale and model wake data, in the form of wake profiles at tip speed ratios of 3.3 and 3.7, respectively. The choice of these values was dictated by the availability of a reasonable amount of cross-wake data from the full-scale data set, and the proximity of the tip speed ratios in the two cases. It is seen that the shapes of the model and the full-scale wake are somewhat different. The full-scale wake is wide and has a homogenous central portion, implying significant cross-wake mixing.

The selected analysis procedure for the model wake was aimed at reproducing the inherent time and cross-wake averaging involved in the full-scale measurements. Attempts were also made to simulate the incident mean velocity and turbulence content. The choice of a narrow wind speed range for the construction of the full-scale wake profile minimizes the effect of variations of wind speed with incident wind direction. The most likely explanation for the discrepancy is therefore scale effect.

Despite attempts at similarity, the scales of turbulence in the atmosphere may have been different from those in the water tank of the simulations and have varied according to stability. Large scale inhomogeinities of the terrain impose energetic turbulent motions with characteristic scales of the size of the wake (and even larger), leading to smearing of velocity gradients of the kind found in the centre of the wake (see model wake profiles). However, it may be noted that the slopes of the two wake profiles in Figure 7, in the region of steepest gradient (towards the edge of the wake) are almost identical.

DISCUSSION AND CONCLUSIONS

The results of this study are very encouraging, with regard to the further use of PIV on small-scale models to investigate the fundamental properties of real wind turbines. The wake centreline velocity ratios measured at model scale, and those from the Samos Island experiments, show remarkably good agreement, both in absolute value, and in their relationship to tip speed ratio. Although it would be unwise to draw too many firm conclusions at this stage, bearing in mind the difference in scale of the two experiments, the further use of PIV in this field seems to be clearly indicated. It is inferred that a more careful assessment of the effect of turbulence, in terms of its spectral content rather than its integral levels, on the wake properties is necessary.

A number of investigations suggest themselves. In particular, the study of the change in wake properties in the transition from low to high windspeed (ie. high to low tip speed ratio) is of interest. This work is actually planned, and will be based on further analysis of the turbulence content of the measured wakes. Analysis of wake vorticity, readily available from the PIV vector maps, is also an option being explored. In this case it may be possible to investigate the properties of the wake under conditions where simple analytic models for wind turbine rotors, eg. actuator-disc theory, fail, for example where the rotor is heavily stalled, or where the thrust coefficient exceeds unity.

In these respects, it is hoped that further comparisons of PIV measurements and full scale data will be forthcoming shortly.

ACKNOWLEDGEMENTS

The authors would like to extend their thanks to the following people: Jean-Baptiste Richon and Iain Morrison of Edinburgh University Physics Department, for design of the image shifting system and assessment of image shifting errors, respectively, and John Korsgaard of LM Glasfiber A/S, and Tom Pedersen of Vestas A/S, for supplying details of the WM19S wind turbine and rotor blades.

The University of Athens research group would also like to thank the Greek Ministry of Industry, Energy and Technology for financial support of the Samos experimental campaign.

Finally, both the teams at Athens and Edinburgh would like to express their thanks to the British Council, for funding their ongoing collaboration.

REFERENCES

1. Hogstrom, U., Asimakopoulos, D.N. , Kambezidis, H.D., Helmis, C.G., and Smedman, A., 1988, Atmos. Environ., 22, 803-820.

2. Taylor, G.J., Hojstrup, J., and Luken, E., 1988, Proceedings of the Euroforum- New Energies Congress (Germany), 3, 755-758.

3. Larsen, A., and Velk, P., 1989, EWEC Procd (Glascow, Scotland), 482-487.

4. Nierenberg, R., 1989, EWEC Procd. (Glascow, Scotland).

5. Elliott, D.L., and Barnard, J.C., 1990, Solar Energy, 45, 265-283.

6. Van Der Snoek, L.,1989; EWEC Procd (Glascow, Scotland).

7. Ainslie, J.F., 1987, International Conference on Wind Farms Procd, (Leeuwarden, Netherlands).

8. Papaconstantinou, A., and Bergeles, G., 1988, J. Wind Eng. Ind. Aerodyn., 31,133-146.

9. Taylor, G.J.,1990, "Wake measurements on the NIBE wind-turbines in Denmark. Part 2:data collection and analysis", CEC Contract EN3W.0039.UK(H1).

10. Strickland, J.H., and Goldman, A.L, 1981, J. Energy, 5, 94-98.

11. Infield, D., Grant, I., Smith, G., and Wang, X., 1994, BWEA 16 Procd. (Stirling, Scotland).

12. Whale, J., and Anderson, C.G., 1993, ECWECs Procd, Lubeck-Travemunde, Germany, 8-12 March.

13. Helmis, C.G., Asimakopoulos, D.N., Papadopoulos, K.H., Papageorgas, P.G., Soilemes, A.T., and Kambezidis, H.D., 1993, ISES Solar World Congress Procd, 8, 287-292.

14. Gray, C., Greated, C.A., McCluskey, D.R., and Easson, W.J., 1991, J. Phys.: Meas. and Sci. Tech., 2, 717-724.

15. Helmis, C.G., Papadopoulos, K.H., Soilemes, A.T., Papageorgas, P.G. and Asimakopoulos, D.N., 1993, BWEA 15 Procd, 99-104.

COLUMN 1 TEXT START

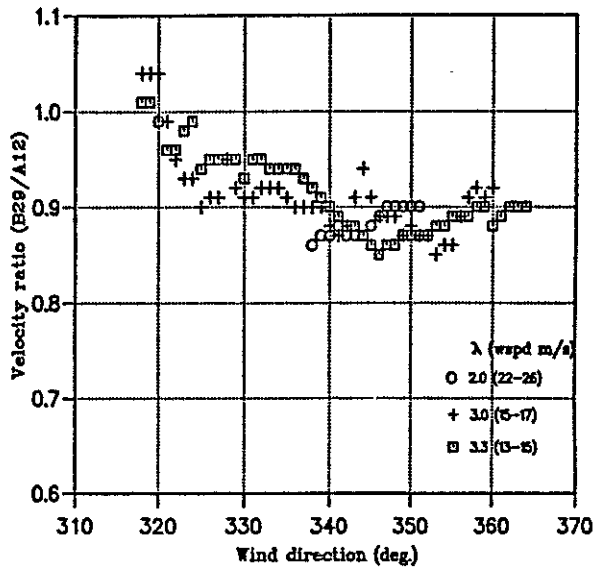

Figure 1 Non-wake data at 1.1D (turbine stationary) from full-scale measurements

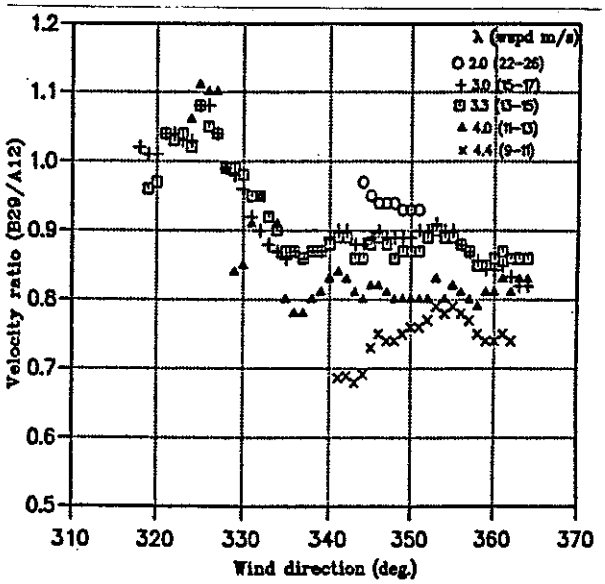

Figure 2 Corrected wake data at 1.1D (turbine operational) from full-scale measurements

TERMINATION OF COLUMN 1

COLUMN 2 TEXT START

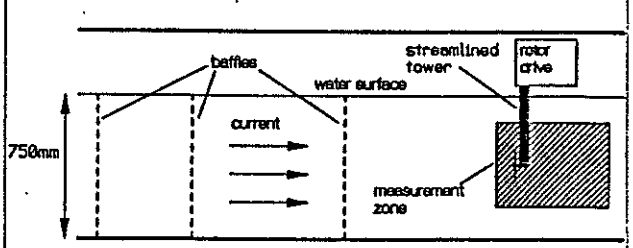

Figure 3 Schematic diagram of PIV set-up in the laboratory

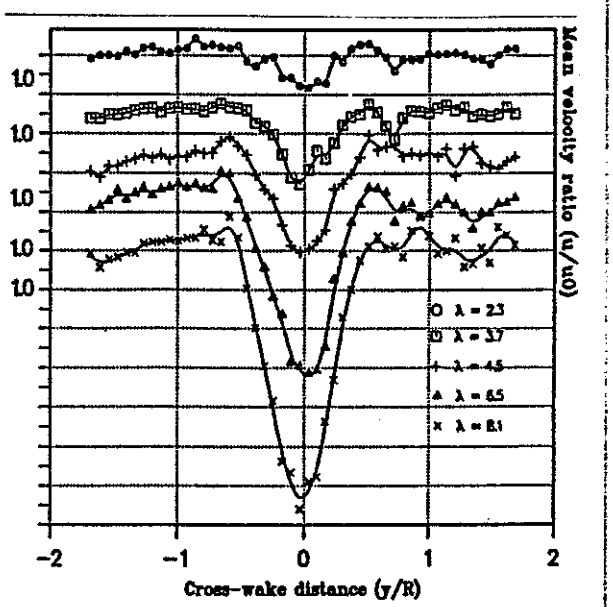

Figure 5 Wake velocity profiles at 1.1D from PIV experiments

TERMINATION OF COLUMN 2

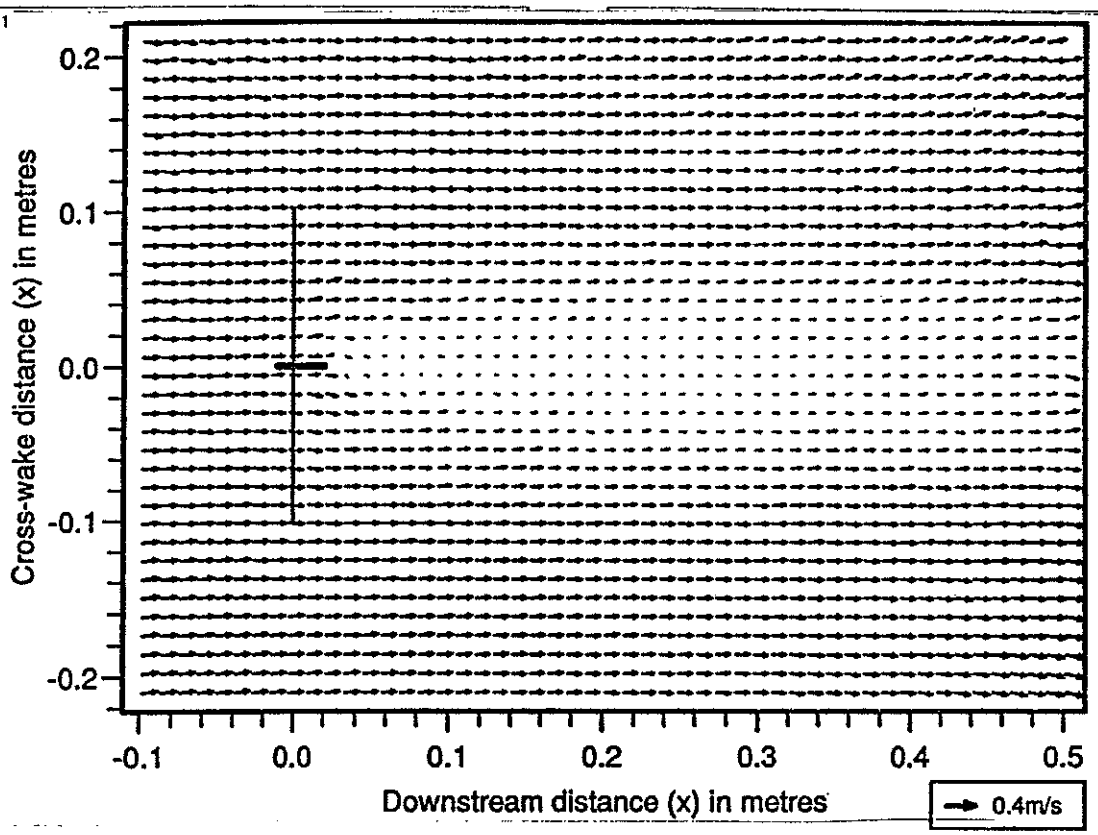

Figure 4 PIV velocity vector map of wake behind model rotor at λ=6.5

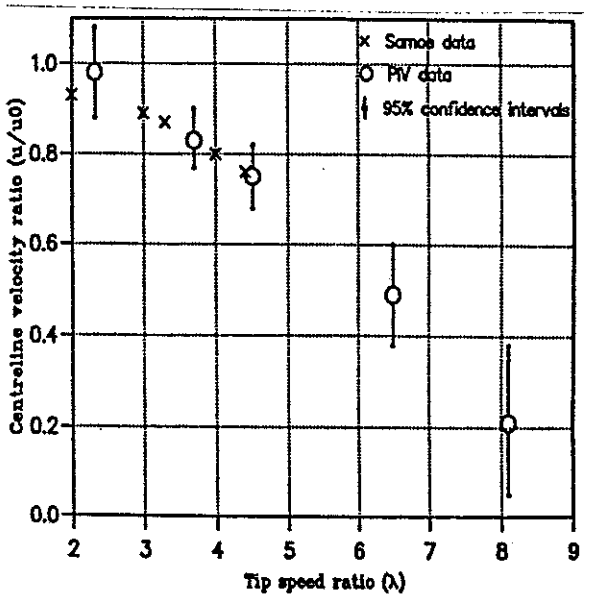

Figure 6 Comparison of centreline velocity ratios at 1.1D between full-scale and PIV data

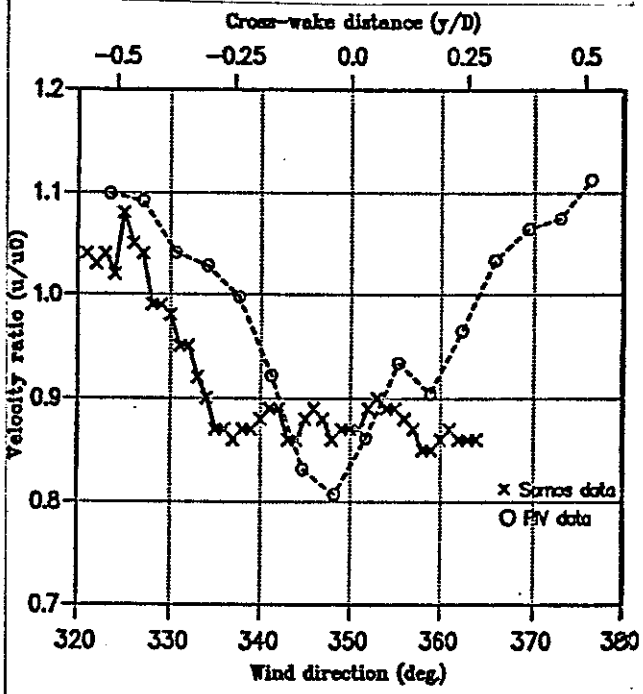

Figure 7 Comparison of wake velocity profiles at 1.1D between full-scale (λ=3.3) and PIV data (λ=3.7)